Polymer 51 (2010) 1147–1155

Contents lists available at ScienceDirect

Polymer

journal homepage: www.elsevier.com/locate/polymer

Effect of nanosilica on the co-continuous morphology of polypropylene/polyolefin elastomer blends

S.H. Lee [a], M. Kontopoulou [a,*], C.B. Park [b]

[a] Department of Chemical Engineering, Queen's University, Kingston, ON K7L3N6, Canada
[b] Department of Mechanical and Industrial Engineering, University of Toronto, Toronto, ON M5S3G8, Canada

ARTICLE INFO

Article history:
Received 25 October 2009
Received in revised form
8 January 2010
Accepted 11 January 2010
Available online 18 January 2010

Keywords:
Nanocomposites
Thermoplastic Olefin blends
Co-continuous morphology

ABSTRACT

This paper reports the effect of nanosilica (SiO_2) on the morphology of co-continuous immiscible polypropylene (PP)/polyolefin elastomer (POE) blends. The unfilled blends display phase inversion and a co-continuous structure at a ratio of 50/50 PP/POE by weight. Upon addition of SiO_2 in the presence of maleated PP compatibilizer a finer structure, consisting of elongated POE particles dispersed within the PP phase is obtained. This transformation is associated to the presence of finely dispersed SiO_2 particles that are localized exclusively within the PP matrix. The impact properties, flexural and Young's moduli of the blends increase significantly, pointing to a synergistic effect arising from the presence of the reinforced PP phase, containing high amounts of the finely dispersed elastomeric phase.

1. Introduction

Polymer blending is used extensively to develop new materials that exhibit a favorable combination of properties, depending on the selection of blend components. As most polymers are immiscible, their blends form multi-phase systems with various morphologies and synergistic properties. The nature of the structures created during processing depends upon several factors, such as the material properties of the neat polymers (interfacial tension, rheological properties), processing conditions (shear rate and mixing time) and the relative amounts of material used. The type of morphology determines to a large extent the physical properties of the blends, thus proper control of the morphology plays a key role in inducing desirable properties to the blends. The droplet/matrix morphology, which imparts favorable impact and other mechanical properties, as in the case of high-impact polystyrene and polypropylene, has been widely studied. Co-continuous morphologies have also drawn significant interest [1], because they have the potential to widen the application range for polymer blends due to their interconnected nature [1–4]. Co-continuous morphologies exhibit interesting properties relevant to conductivity or permeability owing to the percolation of the two phases. A wide range of techniques to determine the co-continuity region and the resulting structures, including solvent extraction [5–9], microscopy [10–14] and rheology [10,15–17] have been described in the literature.

Extensive research during the last decade has confirmed the influence of nanoparticle addition on the morphology of polymer blends. It is now widely accepted that in the presence of nanoparticles, such as organoclays and nanosilica, the droplet-matrix morphology shifts toward a finer dispersion of the minor phase. The selective localization of the nanofiller in one of the phases, typically the matrix or the interphase, seems to be key to explaining this phenomenon. Possible explanations that have been offered include compatibilizing effects due to filler adsorption at the interface of the two polymers, resulting in a reduction in the interfacial tension [18–20]. However these mechanisms are obviously not dominant when the filler resides in the matrix [21]. In that case it has been speculated that exfoliated clay platelets or well dispersed nanoparticles surrounded by an immobilized bound layer of polymer may hinder particle coalescence by acting as physical barriers [22–24].

On the other hand, there are quite a few reports of nanofillers favoring the formation of co-continuous structures in various blend combinations [25–30]. In some cases, the formation of a double-percolated structure, where conductive fillers such as carbon nanotubes are dispersed in one of the co-continuous phases is desirable and is done on purpose, since it can result in favorable conductive properties [31,32]. It is therefore clear that, apart from the obvious effect that nanofillers have on the physical properties of the blends, they can also generate a more indirect effect, through the control of their morphology.

* Corresponding author. Tel.: +1 613 533 3079; fax: +1 613 533 6637.
E-mail address: marianna.kontopoulou@chee.queensu.ca (M. Kontopoulou).

0032-3861/$ – see front matter © 2010 Elsevier Ltd. All rights reserved.
doi:10.1016/j.polymer.2010.01.018

Fig. 1. TSE screw configuration.

The effects of nanosilica on thermoplastic olefin (TPO) blends comprised of polypropylene and ethylene-α-olefin copolymer-based polyolefin elastomers (POEs) have been investigated, in the context of the selective localization of nanosilica in the PP matrix [33,34]. This approach has been shown to impart improved stiffness, while preserving the ductility of the blend. Additionally it has been shown that the droplet-matrix morphology of these blends appears finer, when nanosilica is localized in the PP matrix [33,34]. The present work focuses on co-continuous PP/POE blends and reports the effect of nanosilica on the co-continuous structure, at the phase inversion composition. The implications of the structural changes on the physical performance of the blends have been investigated.

2. Experimental

2.1. Materials

Polypropylene homopolymer (PP), Escorene® PP 1042, MFR 1.9 g/10 min at 230 °C, was supplied by ExxonMobil Chemical. Maleated PP (PP-g-MAn), Fusabond® PM 613, with MFR 49 g/10 min (measured at 230 °C) containing 0.55 wt% of maleic anhydride was supplied by E.I. DuPont Canada. The polyolefin elastomer (POE) was a single-site catalyzed poly(ethylene-*co*-octene) (Engage™ 8100), containing 24 wt% of comonomer with density of 0.87 g/cm^3 and melt flow index of 1.0 g/10 min (measured at 190 °C) and was provided by Dow Chemical. A fumed nanosilica grade Aerosil® R805 (SiO_2), surface modified with octylsilane, having a specific surface of 150 ± 25 m^2/g and a mean particle size of 12 nm, was supplied by Evonik Industries (formerly Degussa Corporation). Irganox 225 antioxidant was obtained from Ciba-Geigy.

2.2. Compounding procedure

PP/POE blends containing POE amounts ranging from 10 to 70% by weight were prepared in a Werner Pfleiderer ZSK-30 ($L/D = 40$, $D = 30.7$ mm) co-rotating twin screw extruder (TSE) using the screw configuration shown in Fig. 1. The screw was configured with

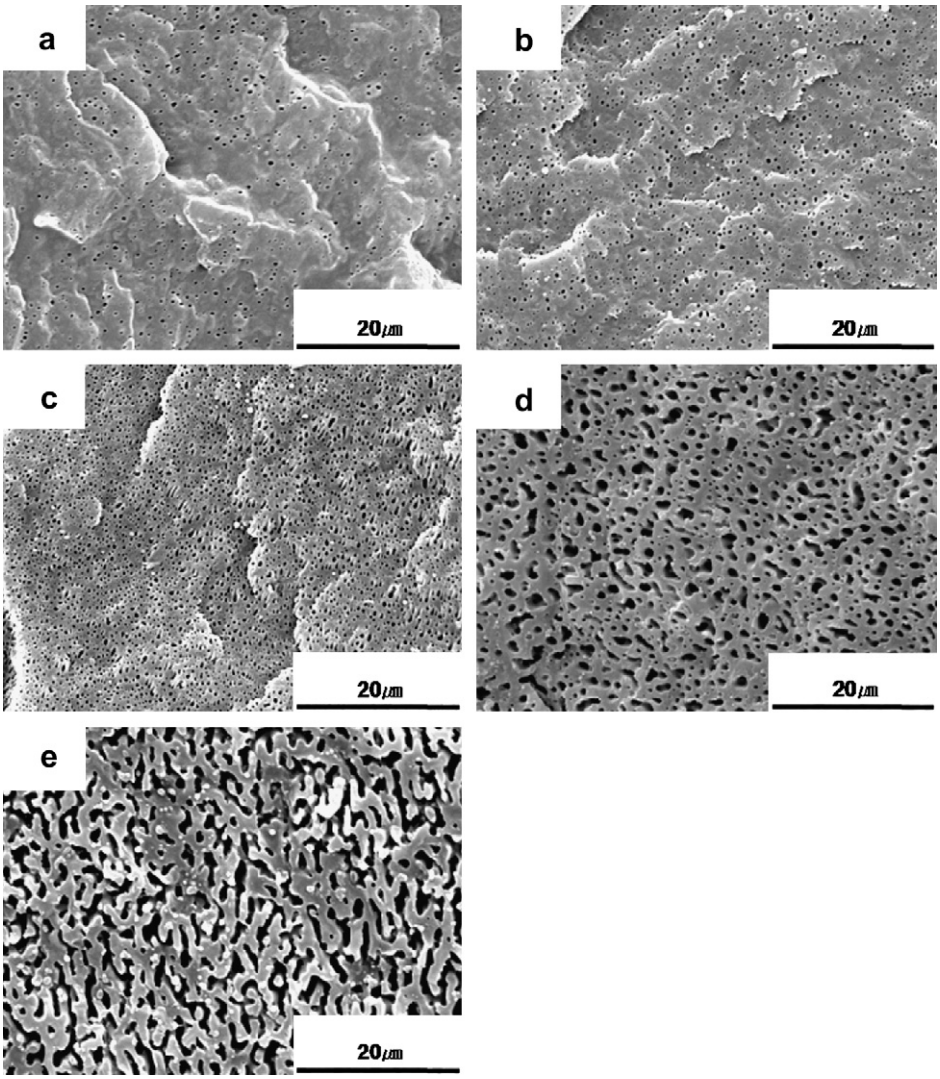

Fig. 2. SEM micrographs of etched surfaces of PP/POE blends. The ratios of PP/POE are (a) 90/10; (b) 80/20; (c) 70/30; (d) 60/40; (e) 50/50. The darker domains correspond to the etched POE phase.

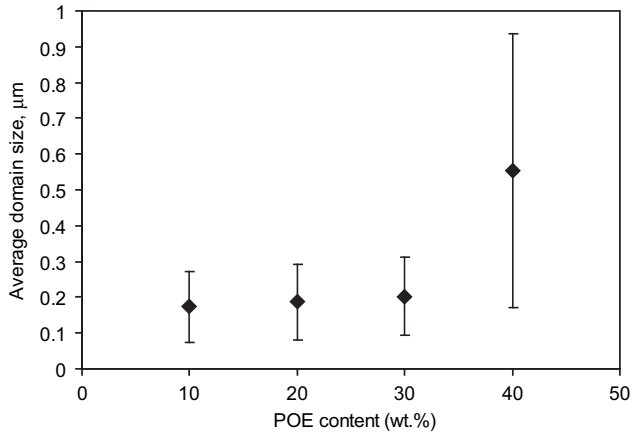

Fig. 3. Average POE domain size as a function of POE content. Error bars represent the standard deviation.

four blocks of kneading discs having positive (+30°), neutral (90°), and negative (−30°) staggered angles and two left-handed screw elements, to provide good dispersive and distributive mixing. The screw speed was 200 rpm, resulting in an extrusion rate of 2.5 kg/h. The temperature profile in the extruder from the feeding section to the die was 60 °C–200 °C–205 °C–205 °C–210 °C–210 °C–200 °C for all blends. These conditions were selected because prior work has shown that they provide the optimum dispersion of nanosilica.

Silica was added to the 50/50 PP/POE blends at loadings ranging from 1 to 5 wt%. PP-g-MAn was used to improve the dispersion of SiO_2 resulting in a PP matrix composition of PP/PP-g-MAn 90/10. Antioxidant (0.3 phr) was added to all formulations.

2.3. Mechanical properties

Tensile properties were measured using an Instron 3369 universal tester, at crosshead speeds of 50 mm/min. Dumbbell-shaped specimens were cut with a Type V die according to ASTM D638 from 1.5 mm thick sheets, which were prepared by compression molding of the compounded samples at approximately 200 °C using a Carver press.

Flexural tests were performed according to ASTM D790, procedure B, at a speed of 13.65 mm/min. Rectangular bars of dimensions 127 × 12.7 × 3.2 mm were produced by compression molding at 200 °C. Notched Izod impact tests were carried out using an Instron BLI impact tester at room temperature according to ASTM D 256. Specimens of dimensions 64 × 12.7 × 3.2 mm were prepared by compression molding at 200 °C. At least 5 specimens were tested for each sample and the average values are reported.

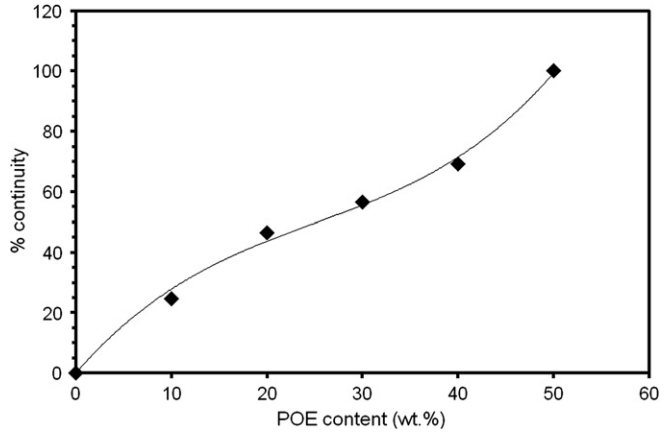

Fig. 4. Percentage of continuity of the POE phase as a function of POE content.

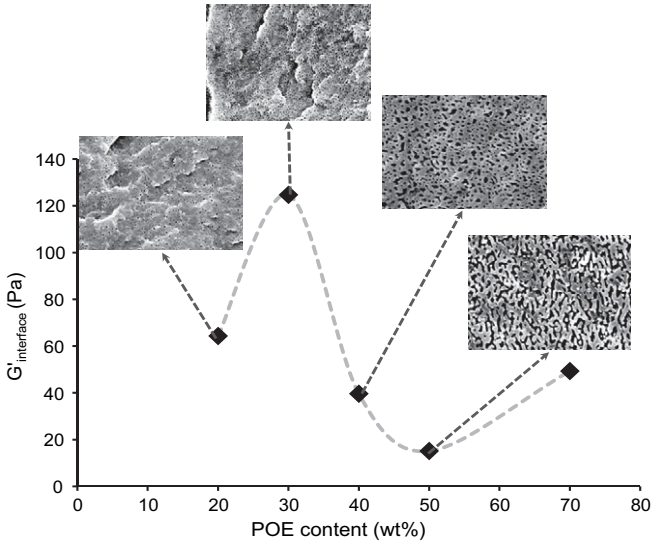

Fig. 5. $G'_{interface}$ as a function of POE content at 0.04 rad/s and 190 °C.

2.4. Microscopy and image analysis

The state of dispersion of the filler was assessed by TEM imaging, using an FEI Tecnai 20 instrument. Ultra-thin sections were cryomicrotomed using a Leica ultra microtome and stained in RuO_4 vapor to enhance the phase contrast between the PP and elastomer phases. For SEM observations, samples were first hot pressed at 190 °C, 2 tons for 1 min, then immersed in liquid nitrogen for 5 min before brittle fracture. The elastomer phase was etched in n-heptane for 2.5 h at 80 °C. The etched surfaces were observed on a JEOL JSM-840 scanning electron microscope. The SEM images were analyzed by using the Sigma Scan Pro image analysis software to estimate the average diameters of the dispersed elastomer phase on the basis of the Ferret diameter, which is calculated based on the estimated area, *A*, of the particles, according to:

$$D = \sqrt{\frac{4A}{\pi}} \tag{1}$$

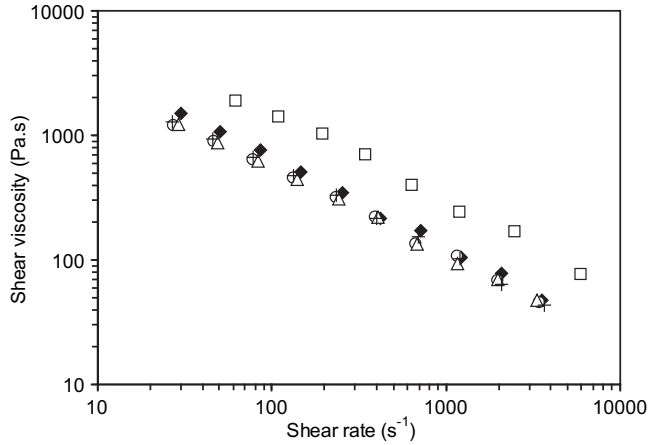

Fig. 6. Shear viscosities of blend components as a function of shear rate at 200 °C. (◆) PP; (□) POE; (○) PP/PP-g-MAn; (△) PP/PP-g-MAn/SiO_2 2 wt%; (+) PP/PP-g-MAn/SiO_2 10.5 wt%.

Table 1
Shear viscosity data and model predictions for the phase inversion compositions of the PP/POE blends and composites containing 5 wt% SiO_2, at various shear rates.

Shear rate (s^{-1})	η_{PP} (Pa.s)	η_{POE} (Pa.s)	$\eta_{PP/PP\text{-}g\text{-}MAn+silica}$ (Pa.s)	ϕ_{POE} of PP/POE[a]	ϕ_{POE} of (PP/PP-g-MAn)/POE with 5 wt% SiO_2[a]
20	2098	4699	1637	0.53	0.56
50	1084	2456	862	0.53	0.55
100	658	1504	531	0.53	0.55
200	400	920	327	0.53	0.55
500	207	481	172	0.53	0.55

[a] Obtained from equation (4).

2.5. Rheological characterization

Rheological characterization was carried out using a Reologica ViscoTech oscillatory rheometer using 20 mm parallel plate fixtures, with a gap of 1 mm at 190 °C, under nitrogen blanket. The rheometer was operated in the dynamic oscillatory mode in the linear viscoelasticity region. The complex viscosity (η^*), storage modulus (G') and tan δ were measured as a function of angular frequency (ω). Time-sweep experiments were performed using the same instrument, at a frequency of 0.1 Hz and constant strain of 2%.

Steady-shear viscosity measurements were done using a Rosand RH2000 Dual Bore Capillary rheometer at a temperature of 200 °C. The Bagley and Rabinowitch corrections were applied.

2.6. Annealing

Annealing tests were carried out using a hot stage at 190 °C. Samples were annealed for different periods of time ranging from 1 to 60 min and were quenched subsequently in cold water.

2.7. Solvent extraction

The selective solvent dissolution technique was employed to determine the co-continuity region. This technique is widely employed and has been described in detail previously [5–9]. The selected solvent to dissolve the POE phase was n-heptane. Samples weighing approximately 1 g of a compact sample were weighed then immersed in 50 mL of solvent during 2.5 h at 80 °C. After the dissolution process was complete, the remaining parts of the sample were dried under vacuum at 60 °C for 24 h, and then weighed again. The continuity of one phase can be defined as the fraction of polymer that belongs to a continuous phase [35]. For a polymer A, this parameter is evaluated from the following expression:

$$\%\ \text{continuity of } A = \frac{m_{\text{initial}}(\text{sample}) - m_{\text{final}}(\text{sample})}{w(A) \times m_{\text{initial}}(\text{sample})} \times 100 \quad (2)$$

where $w(A)$ is the weight fraction of A in the initial blend. Ideally the dissolution process should be used to dissolve each individual phase, using an appropriate solvent. When the percentage of continuity of both components equals 100%, the morphology of the blend is considered to be co-continuous. However in the present work it was impossible to find a solvent that will selectively dissolve PP without affecting the POE phase, therefore the technique was only carried out for the POE component.

3. Results and discussion

3.1. Unfilled PP/POE blends

We begin our investigation from the unfilled PP/POE blend, which will provide a basis for comparison with the nanocomposite blends. This is a thermodynamically immiscible system in the range of compositions investigated in the present work, as reported previously by numerous researchers [36,37]. Fig. 2 shows SEM images of blends containing various amounts of POE. The number average diameters (D_n) of the dispersed phase droplets as a function of the POE content are shown in Fig. 3. The corresponding co-continuity diagram obtained by selective solvent extraction of the POE phase via equation (2) is presented in Fig. 4. The increase in continuity above 20 wt% corresponds to the coarsening of the structure, due to the coalescence of POE droplets that takes place between 30 wt% and 40 wt% POE (Fig. 2(c) and (d)). A fully co-continuous structure is obtained at 50 wt% POE (see also Fig. 2(e)).

The rheological properties of immiscible blends are sensitive to both their composition and their morphology. Blends having a droplet/matrix morphology display a characteristic relaxation process in the long time range, leading to an enhancement of the storage modulus G' at low frequencies during shear oscillatory deformation. This additional process is attributed to the shape relaxation of the deformed droplets, which is mainly driven by the interfacial tension [38–40] and can be modeled using the Palierne emulsion model [41]. In contrast, the shape relaxation of co-continuous morphologies is less visible, resulting in reduced elasticity.

The storage modulus of the blends, G'_{blend}, is plotted as a function of composition in Fig. 5. To improve the comparison and to highlight the excess elasticity due to shape relaxation, the compositional effect was subtracted. For this purpose the Gramespacher and Meissner model was used [42]. This model

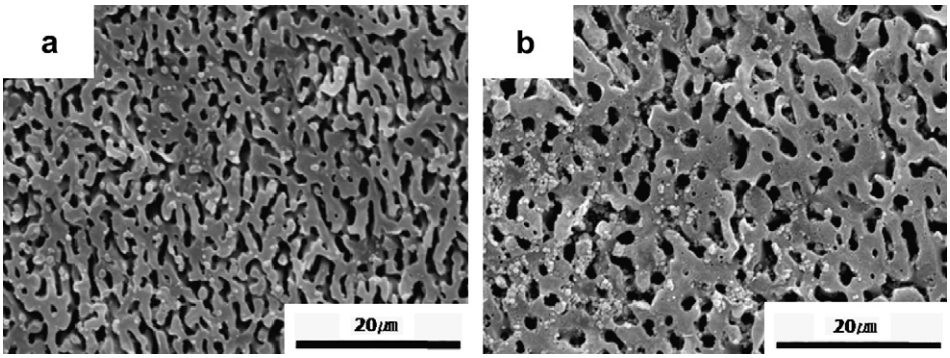

Fig. 7. Morphology of 50/50 PP/POE blend and composite (a) PP/POE; (b) PP/POE/5 wt% SiO_2.

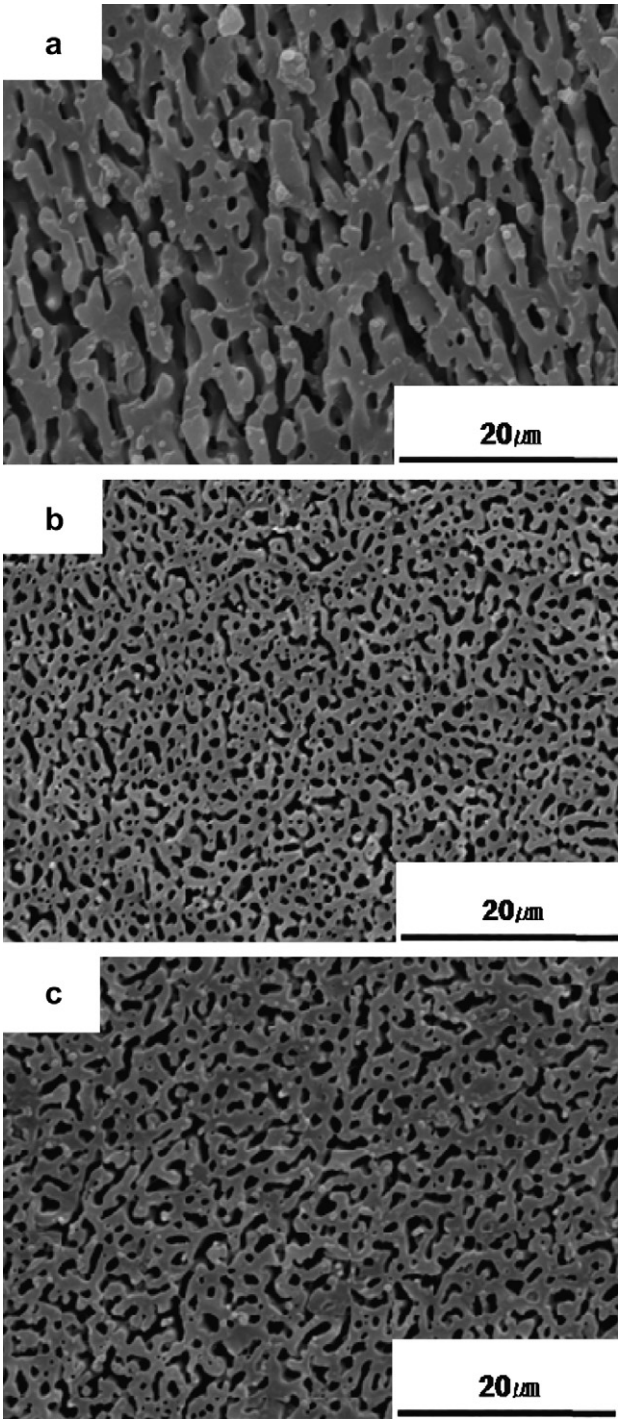

Fig. 8. SEM micrographs of (PP/PP-g-MAn 90/10)/POE 50/50 composites after POE extraction: (a) 0 wt% SiO_2; (b) 1 wt% SiO_2; (c) 5 wt% SiO_2. Scale bars represent 20 μm.

describes the frequency-dependent behaviour of the complex modulus of an immiscible blend by considering the contributions attributed to the viscoelastic properties of the components plus the contribution caused by the interfacial tension between the components. Using a simple mixing rule, the elastic modulus, G'_{blend}, of the PP/POE blends can be written:

$$G'_{blend} = \phi G'_{POE} + (1-\phi)G'_{PP} + G'_{interface} \quad (3)$$

where ϕ is the volume fraction of the dispersed phase. Using the experimental data obtained for the blend and the individual components, the contribution caused by the interfacial tension $G'_{interface}$ between the two components has been calculated using equation (3) and is plotted in Fig. 5. The morphologies obtained by extraction are also overlaid in Fig. 5. As shown in Fig. 5, In the presence of finely dispersed POE droplets, at POE fractions between 20 and 30%, the storage modulus increased significantly. Coalescence occurred above 30 wt% POE, resulting in a decrease in the interfacial area, reflected by a decrease in the storage modulus. A further decrease of the storage modulus is correlated with the creation of continuity of the POE phase. At around 70 wt% POE content, a droplet-matrix morphology has been re-established, this time with POE being the continuous phase, thus the value of the elastic contribution due to the interfacial tension shows an increasing tendency.

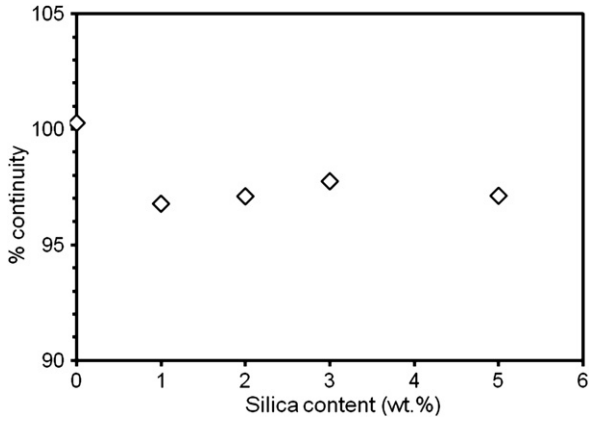

Fig. 9. Percentage of continuity of the POE phase as a function of silica content for the (PP/PP-g-MAn 90/10)/POE 50/50 blend.

As seen in Fig. 2 and inferred from Figs. 4 and 5, phase inversion takes place at about 50/50 PP/POE ratio by weight. This finding can be compared to theoretical predictions of the phase inversion composition that can be obtained by using various theoretical models, based on the values of the shear viscosities of the individual components [1,43]. The shear viscosities of the PP and POE components measured by a capillary rheometer are shown in Fig. 6 and summarized in Table 1. Given the uncertainty that exists in the estimation of the shear rates inside the TSE, a range of shear rates is provided in Table 1. As seen in Table 1, the viscosity ratio η_{POE}/η_{PP} of the polymers used in this work is around 2 throughout the range of shear rates tested. For this viscosity ratio the correlation suggested by Kitayama et al. [44] (equation (4)) was the most successful in predicting phase inversion at a composition of 53 wt% POE.

$$\frac{\phi_1}{\phi_2} = 0.887\left[\frac{\eta(\dot{\gamma})_1}{\eta(\dot{\gamma})_2}\right]^{0.3} \quad (4)$$

where 1: POE phase, 2: PP phase.

3.2. Effect of nanosilica on the co-continuous morphology

Upon addition of 5 wt% SiO_2 to the PP/POE blend the co-continuous structure of the blends appeared relatively unchanged, albeit slightly coarser (Fig. 7). It has been shown previously that in the absence of a compatibilizer the dispersion of SiO_2 in these blends is rather poor and that addition of PP-g-MAn results in a significant improvement in the filler dispersion [33]. Therefore blends containing 10 wt% of PP-g-MAn compatibilizer in the PP matrix, so that the matrix consisted of a 90/10 by weight ratio PP/PP-g-MAn were prepared. The overall composition of the rigid/elastomeric components in the blends was always maintained at 50/50 for proper comparison.

In the presence of PP-g-MAn the unfilled blends maintained a co-continuous morphology, as shown in Fig. 8(a), meaning that the slight reduction in viscosity in the presence of the low molecular weight PP-g-MAn did not affect significantly the phase inversion composition. Fig. 8(b) and (c) depicts a transformation to a much finer morphology upon addition of SiO_2, consisting of elongated domains of the POE phase, intimately interdispersed with the PP phase. The resulting structure resembles more the one obtained previously for the 60/40 PP/POE unfilled blends (Fig. 2d). The percent continuity in the blend dropped slightly as revealed by the extraction experiments (Fig. 9). Given the uncertainty that is inherently involved in the extraction experiments [14], TEM imaging was also used to confirm this transformation (Fig. 10). TEM images further revealed that the finely dispersed SiO_2 particles were located exclusively in the PP/PP-g-MAn matrix. This is consistent with our previous findings on PP/POE/nanosilica blends [33,34]. On the basis of thermodynamic arguments, taking into account the values of interfacial tensions between the surface modified silica and the PP and POE phases, it has been shown that silica modified with octylsilane has a greater affinity toward the PP phase [34].

The elastic moduli of the nanocomposite blends measured at low frequencies provide further evidence of the morphological changes (Fig. 11). It should be noted that in addition to the compositional and interfacial effects, the value of the elastic modulus is also influenced significantly by the presence of the nanofiller. Therefore for this evaluation equation (3) was used again, but in this case, instead of the G′ of the PP matrix, the G' of the 90/10 PP/PP-g-MAn matrix containing the equivalent amount of SiO_2 was measured, by compounding the appropriate composites. The results show that $G'_{interphase}$ calculated through equation (3) by replacing G_{PP}' by $G'_{(PP/PP\text{-}g\text{-}MAn/silica)}$, increases at SiO_2 contents above 1 wt%, confirming an enhanced interfacial contribution.

Based on the above evidence, we conclude that a morphological transformation takes place at the phase inversion composition upon addition of finely dispersed nanosilica particles, which are selectively localized in one phase. The PP component containing the nanoparticles tends to become the continuous phase as the SiO_2 loading increases.

The morphological stability of the unfilled blends and composites was examined through annealing experiments, using a hot stage. The morphology of the co-continuous (PP/PP-g-MA 90/10)/POE 50/50 blend annealed at various times is shown in Fig. 12a. Significant coarsening was observed with increasing annealing time. This is further reflected in time-sweep experiments,

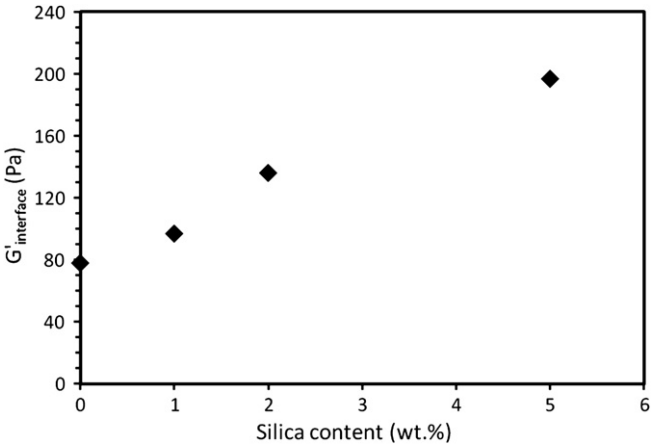

Fig. 11. $G'_{interface}$ as a function of silica content for (PP/POE 50/50)/silica composites at 0.04 rad/s and 190 °C.

shown in Fig. 13, which clearly show that the elastic modulus of the unfilled blend dropped with time, signifying a reduction in the interfacial area between the two phases. This is in agreement with findings by Vinckier and Laun [45] and Mekhilef et al. [46] who noted the coarsening process of co-continuous structures by microscopy and rheological characterization.

For the silica filled blends, the micrographs in Fig. 12b and c similarly show significant coarsening upon annealing, manifested by a significant increase in the dispersed droplet diameter. It is interesting however to note that the PP matrix still continues to form a continuous phase. The corresponding time sweeps of the filled composites show an initial decrease representative of the coarsening, followed by further increases in G' as a function of time, which may arise from nanosilica particle aggregation phenomena [47]. This implies that different mechanisms may be affecting the evolution of the rheological properties during the coarsening process in the filled blends.

3.3. Mechanical properties

It is well known that addition of nanosilica results in a significant increase in the Young's and flexural moduli. In our previous work we have demonstrated that when silica is localized in the rigid PP matrix, the elongation at break and impact properties of

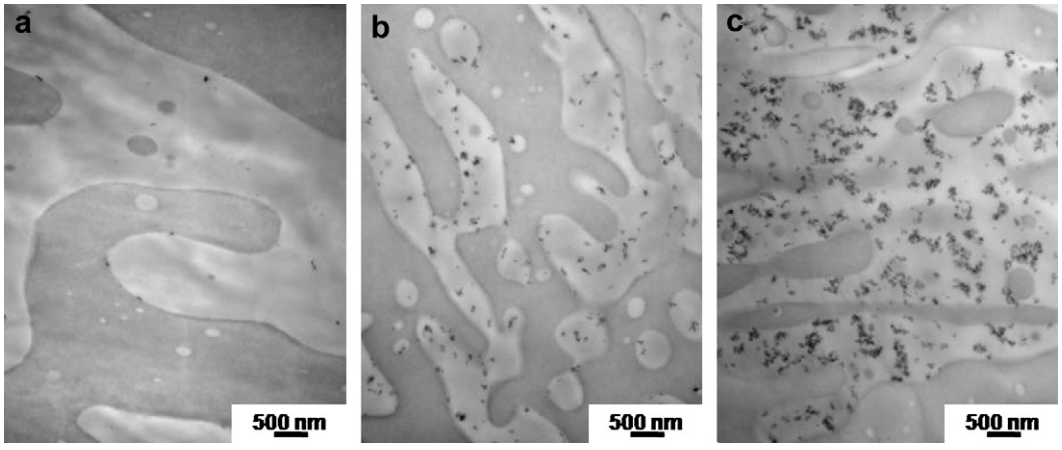

Fig. 10. TEM images of (PP/PP-g-MAn 90/10)/POE 50/50 composites (a) 0 wt% SiO_2; (b) 1 wt% SiO_2; (c) 5 wt% SiO_2. Scale bar: 500 nm. Dark domains represent the stained POE phase.

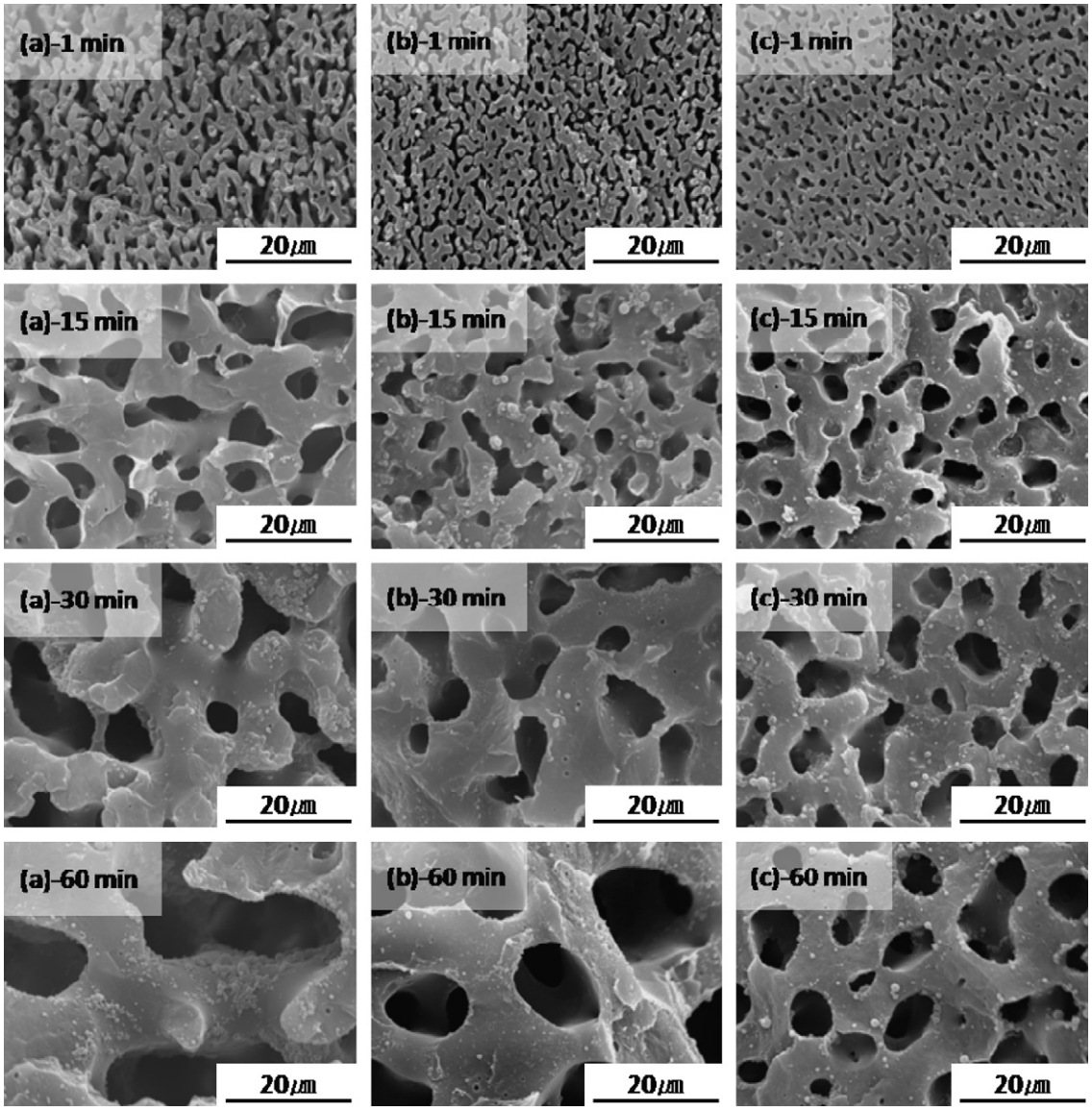

Fig. 12. SEM micrographs of the PP/POE 50/50 blends annealed at various times; (a) unfilled blend, (b) 1 wt% SiO_2, (c) 5 wt% SiO_2.

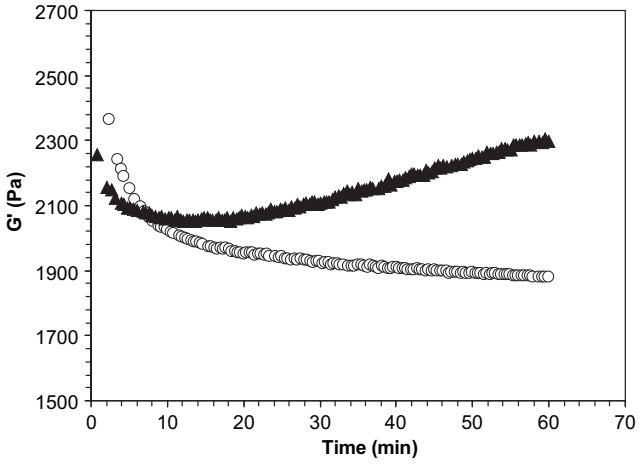

Fig. 13. Time sweeps of the unfilled PP/POE blend and the composite containing 1 wt% silica, at 0.1 Hz, 2% strain and 190 °C; (○) (PP/PP-g-MAn 90/10)/POE 50/50; (▲) (PP/PP-g-MAn 90/10)/POE with 1 wt% SiO_2.

the composites remain unaffected [33,48]. These changes have been attributed to the reinforcement effect of the nanosilica fillers, while the ability of the unfilled elastomeric component to act as impact modifier is maintained.

In this work, in addition to the expected reinforcement effect, an interesting differentiation in the shape of the tensile curves can be observed in Fig. 14. The stress–strain curve of the unfilled 50/50 PP/POE blend has a shape that is typical of an elastomeric response, with the absence of a yield stress. This is expected because this blend is in the vicinity of phase inversion and elastomeric properties likely dominate. However at silica loadings above 1 wt%, the onset of a yield stress becomes apparent and the Young's modulus increases significantly (see also Table 2). In addition to the effect of the filler, this observation may also be attributed to the change in the morphology, which tends toward a continuous rigid PP phase.

Impact properties also show a substantial increase upon addition of the nanosilica (Fig. 15). This is could be attributed to the transformation in morphology, wherein elongated domains of the unfilled elastomeric component are interdispersed with the PP phase, resulting in very high interfacial area, thus improved capability for stress transfer between the two phases.

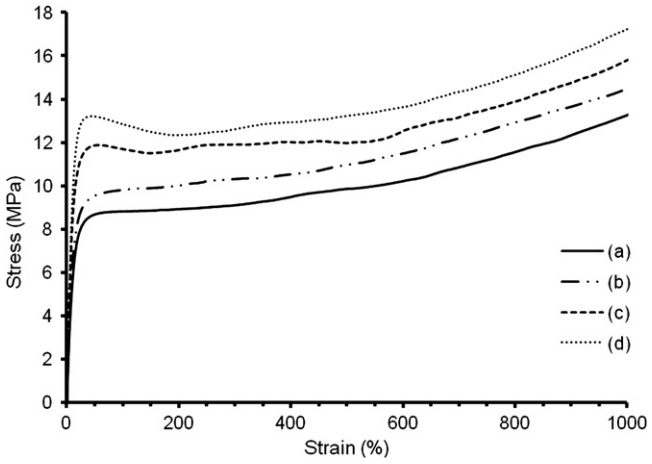

Fig. 14. Tensile curves of (PP/PP-g-MAn 90/10)/POE 50/50 blends with various amounts of silica. (a) PP/POE 50/50; (b) (PP/PP-g-MAn 90/10)/POE 50/50; (c) (PP/PP-g-MAn 90/10)/POE/SiO_2 2 wt%; (d) (PP/PP-g-MAn 90/10)/POE/SiO_2 5 wt%.

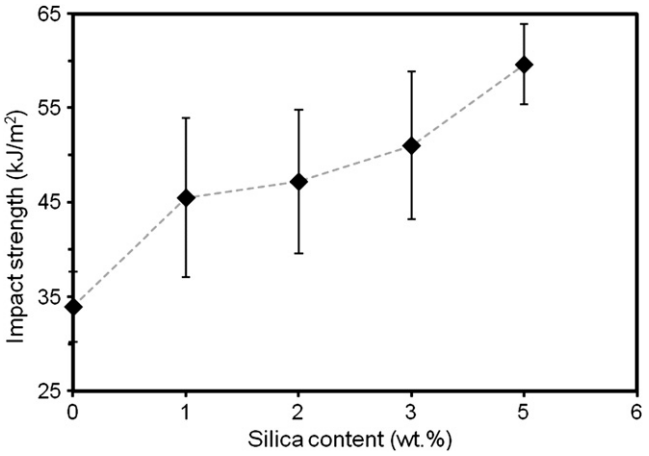

Fig. 15. Notched Izod impact strength for the (PP/PP-g-MAn 90/10)/POE 50/50 blend as a function of SiO_2 content. Error bars represent the standard deviation.

4. Discussion

Based on the results presented above it can be concluded that besides the well-known reinforcement effects of nanosilica, its addition to PP/POE blends in the vicinity of phase inversion results in a favorable transformation of the morphology. The composite structure, which maintains high levels of continuity, is comprised of a reinforced silica/filled PP matrix containing very high amounts of elongated domains of the elastomeric phase. The high interfacial area between the phases results in a significant toughening effect, while the rigidity of the matrix is maintained.

It can be easily argued that the morphological changes are attributed to a compositional effect. A 50/50 (PP + PP-g-MAn)/POE blend containing 5 wt% silica that is exclusively localized in the PP phase, actually corresponds to a blend containing 47.5 wt% of the dispersed POE phase, meaning that a relatively smaller amount of the dispersed phase is contained in the blend. However the change in morphology is also seen for the blends containing just 1 wt% silica, where the shift in composition is minimal.

Changes in morphology in the presence of nanoparticles, including finer dispersion of the minor phase, and appearance of co-continuous morphologies have been widely reported in the literature [18–30]. The appearance of co-continuous morphologies has been discussed in the context of bulk continuum properties, such as altered viscosity ratios in the presence of nanoparticles [25,26]. Fig. 6 shows the dependence of the shear viscosity on shear rate of all blend components. Given that the composite blends consist of a PP/PP-g-MAn/SiO_2 matrix and the unfilled POE, the viscosities of the 90/10 PP/PP-g-MAn matrix containing the equivalent amount of SiO_2 are reported in Fig. 6. It is clear that the shear viscosity of the composites at high shear rates, which are relevant to compounding, remains virtually unaffected in the presence of the filler, meaning that the viscosity ratios are similar to those of the unfilled blend, resulting in essentially identical phase inversion compositions (see Table 1). Higher elasticity of the matrix may also tend to destabilize the dispersed phase droplets, making them break at lower capillary numbers [49] and to influence the compositions at phase inversion [10]. However changes in matrix elasticity of the nanosilica-filled composites were marginal at the shear rates relevant for compounding, as evidenced by our oscillatory measurements and by the evaluation of entrance pressure drop during the capillary rheometer experiments. Furthermore, given that the nanofillers do not reside at the interface between the two components, interfacial emulsification effects can be excluded.

The remaining explanation is that the competition between break-up and coalescence is altered during compounding. It is likely that in blends filled with rigid nanofillers, droplet break-up is facilitated by the high stresses that develop locally. Additionally, it is obvious from image analysis that the inter-aggregate distances of between 100 and 500 nm, are of similar order of magnitude, or even smaller, than the size of the droplets of the dispersed phase. It can be speculated therefore that the droplets of the dispersed phase are forced to follow a tortuous path, corresponding to conditions of highly confined flow. Blends filled with nanofillers therefore do not follow the well-known bulk dynamics of immiscible polymer blends during shear flow. It has been recently shown that for viscosity ratios above 1, such as the ones encountered in our blends, confinement leads to a shift in the critical capillary number to higher numbers, meaning that droplet break-up is facilitated in shear flow [50]. Thus droplet deformation and break-up may be more highly favored, thus resulting to a shift toward a finer morphology.

Table 2
Mechanical properties of (PP/PP-g-MAn 90/10)/POE 50/50 blends containing various amounts of silica.

Composition		Yield stress (MPa)	Max. tensile stress (MPa)	Elongation at break (%)	Young's modulus (MPa)	Flexural modulus (MPa)	Flexural strength (MPa)
PP/POE	SiO_2 (wt%)						
50[a]/50	0	–	27.8 ± 1.9	2201 ± 153	75 ± 7	137 ± 4	5.7 ± 0.5
	1	–	24.7 ± 4.0	2018 ± 341	81 ± 5	152 ± 23	6.3 ± 0.9
	2	11.7 ± 0.5	29.8 ± 3.2	2179 ± 178	97 ± 9	166 ± 10	6.9 ± 0.3
	3	11.4 ± 0.4	30.7 ± 2.2	2250 ± 128	107 ± 7	164 ± 16	7.2 ± 0.6
	5	13.2 ± 0.2	32.5 ± 0.9	2176 ± 47	114 ± 7	161 ± 18	7.1 ± 0.7

[a] PP matrix composition: PP/PP-g-MAn 90/10.

It has been also widely speculated that rigid nanofillers having a platelet like structure, such as nanoclays, may act to prevent coalescence [22,23,51]. However, since in our silica filled blends coarsening does occur under zero shear conditions, as seen in Fig. 11, coalescence prevention is not the dominant mechanism. Thus the most plausible explanation for the observed changes in morphology is that droplets undergo enhanced deformation and break-up, similar to what is encountered in highly confined flows.

5. Conclusions

Addition of finely dispersed silica in co-continuous blends consisting of PP and ethylene-α-olefin copolymer-based polyolefin elastomers (POEs) resulted in a drop in the amount of continuity and a transformation to a finer morphology, consisting of elongated POE domains inside the PP phase, with the filler residing exclusively in the PP matrix.

Given that the shear viscosity of the filled PP matrix remained virtually unchanged compared to the unfilled polymer at high shear rates relevant to compounding, it was concluded that the change in the morphology was associated with a confinement effect in the presence of the finely dispersed filler, which favors the break-up of the elastomer droplets.

This transformation had profound effects on the mechanical properties of the blends, as they benefited from both the presence of a rigid matrix, as well as high amounts of the elastomeric phase, that were finely interdispersed within the matrix.

Acknowledgements

The authors gratefully acknowledge funding from the Ontario Research Fund (ORF) – Research Excellence (RE) program, by the Ministry of Research and Innovation of Ontario. We would also like to thank Evonik Industries, ExxonMobil, Dow Chemical and E.I. DuPont Canada for providing the materials used in this work.

References

[1] Pötschke P, Paul DR. J Macromol Sci Part C 2003;43(1):87–141.
[2] Gubbels F, Blacher S, Vanlathem E, Jérôme R, Deltour R, Brouers F, et al. Macromolecules 1995;28(5):1559–66.
[3] Willemse RC, Speijer A, Langeraar AE, Posthuma de Boer A. Polymer 1999;40(24):6645–50.
[4] Sarazin P, Favis BD. Biomacromolecules 2003;4(6):1669–79.
[5] Willemse RC, Posthuma de Boer A, van Dam J, Gotsis AD. Polymer 1998;39(24):5879–87.
[6] Willemse RC, Posthuma de Boer A, van Dam J, Gotsis AD. Polymer 1999;40(24):6651–9.
[7] Lyngaae-Jørgensen J. Intern Polym Process 1999;14(3):213–20.
[8] Li J, Ma P, Favis BD. Macromolecules 2002;35(6):2005–16.
[9] Dedecker K, Groeninckx G. Polymer 1998;39(21):4993–5000.
[10] Bourry D, Favis BD. J Polym Sci Part B Polym Phys 1998;36(11):1889–99.
[11] Marin N, Favis BD. Polymer 2002;43(17):4723–31.
[12] Galloway JA, Montminy MD, Macosko CW. Polymer 2002;43(17):4715–22.
[13] Steinmann S, Gronski W, Friedrich C. Polymer 2001;42(15):6619–29.
[14] Galloway JA, Macosko CW. Polym Eng Sci 2004;44(4):714–27.
[15] Ajji A, Choplin L, Prudhomme RE. J Polym Sci Part B Polym Phys 1991;29(13):1573–8.
[16] Mani S, Malone MF, Winter HH. J Rheol 1992;36(8):1625–49.
[17] Steinmann S, Gronski W, Friedrich C. Polymer 2002;43(16):4467–77.
[18] Ray SS, Pouliot S, Bousmina M, Utracki LA. Polymer 2004;45(25):8403–13.
[19] Voulgaris D, Petridis D. Polymer 2002;43(8):2213–8.
[20] Elias L, Fenouillot F, Majeste JC, Cassagnau P. Polymer 2007;48(20):6029–40.
[21] Kontopoulou M, Liu Y, Austin JR, Parent JS. Polymer 2007;48(15):4520–8.
[22] Lee H, Fasulo PD, Rodgers WR, Paul DR. Polymer 2005;46(25):11673–89.
[23] Khatua BB, Lee DJ, Kim HY, Kim JK. Macromolecules 2004;37(7):2454–9.
[24] Austin JR, Kontopoulou M. Polym Eng Sci 2006;46(11):1491–501.
[25] Li Y, Shimizu H. Polymer 2004;45(22):7381–8.
[26] Zhao L, Li Y, Shimizu H. J Nano Nanotech 2009;9(4):2772–6.
[27] Filippone G, Dintcheva NT, Acierno D, La Mantia FP. Polymer 2008;49(5):1312–22.
[28] Wu DF, Wu LF, Zhang M, Zhou WD, Sheng Y. J Polym Sci Part B Polym Phys 2008;46(12):1265–79.
[29] Martin G, Barres C, Sonntag P, Garois N, Cassagnau P. Mater Chem Phys 2009;113(2-3):889–98.
[30] Zou H, Ning NY, Su R, Zhang Q, Fu Q. J Appl Polym Sci 2007;106(4):2238–50.
[31] Pötschke P, Bhattacharyya AR, Janke A. Polymer 2003;44(26):8061–9.
[32] Pötschke P, Kretzschmar B, Janke A. Comput Sci Technol 2007;67(5):855–60.
[33] Liu Y, Kontopoulou M. Polymer 2006;47(22):7731–9.
[34] Bailly M, Kontopoulou M. Polymer 2009;50(11):2472–80.
[35] Pu GW, Luo YW, Lou QC, Li BG. Macromol Rapid Commun 2009;30(2):133–7.
[36] McNally T, McShane P, Nally GM, Murphy WR, Cook M, Miller A. Polymer 2002;43(13):3785–93.
[37] Kontopoulou M, Wang W, Gopakumar TG, Cheung C. Polymer 2003;44(23):7495–504.
[38] Lacroix C, Bousmina M, Carreau PJ, Favis BD, Michel A. Polymer 1996;37(14):2939–47.
[39] Bousmina M, Muller RJ. J Rheol 1993;37(4):663–79.
[40] Friedrich C, Gleinser W, Korat E, Maier D, Weese J. J Rheol 1995;39(6):1411–25.
[41] Palierne JF. Rheol Acta 1990;29(3):204–14.
[42] Gramespacher H, Meissner J. J Rheol 1992;36(6):1127–41.
[43] Omonov TS, Harrats C, Moldenaers P, Groeninckx G. Polymer 2007;48(20):5917–27.
[44] Kitayama N, Keskkula H, Paul DR. Polymer 2000;41(22):8041–52.
[45] Vinckier I, Laun HM. Rheol Acta 1999;38(4):274–86.
[46] Mekhilef N, Favis BD, Carreau PJ. J Polym Sci Part B Polym Phys 1997;35(2):293–308.
[47] Zhang Q, Archer LA. Langmuir 2002;18(26):10435–42.
[48] Liu Y, Kontopoulou M. J Vinyl Add Technol 2007;13(3):147–50.
[49] Mighri F, Carreau PJ, Ajji A. J Rheol 1998;42(6):1477–90.
[50] Vananroye A, Puyvelde PV, Moldenaers P. Langmuir 2006;22(9):3972–4.
[51] Hong JS, Han NK, Ahn KH, Lee SJ, Kim CY. Polymer 2006;47(11):3967–75.